

References

- Biot, M. A., 1956, "Theory of Propagation of Elastic Waves in a Fluid-Saturated Porous Solid," *J. Acoust. Soc. Am.*, Vol. 28, pp. 168-178.
- Bonnet, G., 1987, "Basic Singular Solutions for a Poroelastic Medium in the Dynamic Range," *J. Acoust. Soc. Am.*, Vol. 82, pp. 1758-1762.
- Cheng, A. H. D., and Liggett, J. A., 1984, "Boundary Integral Equation Method for Linear Porous Elasticity with Applications to Soil Consolidation," *Int. J. Numer. Meth. Engng.*, Vol. 20, pp. 255-278.
- Kupradze, V. D., Gegelia, T. G., Basheleishvili, M. O., and Burchuladze, T. V., 1979, *Three-Dimensional Problems of the Mathematical Theory of Elasticity and Thermoelasticity*, North-Holland, Amsterdam, The Netherlands.
- Manolis, G. D., and Beskos, D. E., 1989, "Integral Formulation and Fundamental Solutions of Dynamic Poroelasticity and Thermoelasticity," *Acta Mech.*, Vol. 76, pp. 89-104.

Analysis of the Caustic Method for the Transient Stress Field of Stationary Cracks

Chien-Ching Ma⁹

1 Introduction

In deriving the formula for the method of caustic, several assumptions are made: (a) the specimen is in a plane-stress state; (b) the deformation slope is small; (c) small-scale yielding prevails; (d) the measurements are made within the region of the dominant singular field. These assumptions have been made in most of the subsequent applications of caustics. These restrictions have only recently been investigated and the findings have resulted in the improvement of the validity and accuracy of this method (Rosakis and Ravi-Chandar, 1986; Rosakis and Freund, 1981; Rosakis and Zehnder, 1985).

By analogy with quasi-static fracture, the singular field is expected to dominate the crack-tip stress field at least in the immediate vicinity of the crack tip. The extent of this region of K dominance, however, is not well established particularly under transient conditions. The dynamic stress intensity factor is determined by caustic method from measurements covering a finite region around the crack tip. One must be assured that the K -field does indeed dominate within this region to get good results. In this paper, the validity of the stress singular field is investigated so that measurements of the stress intensity factor using the caustic method are made in the appropriate region with acceptable accuracy. The error in the experimental measurement of the caustics to evaluate the stress intensity factor by assuming that the singular field dominance is investigated. The experimental results of Ravi-Chandar and Knauss (1984) are also discussed in light of this theoretical analysis.

2 Caustic and Initial Curves Due to the Exact Transient Field

The instantaneous value of the dynamic stress intensity factor can be expressed as a function of the maximum transverse diameter D_{\max} of the caustic curve as

$$K(t) = \frac{E}{10.708z_0 d \nu} (D_{\max})^{5/2}. \quad (1)$$

where ν is the Poisson's ratio, E is the elastic modulus, d is the thickness and z_0 is the screen distance.

The dynamic stress intensity factor of a stationary crack subjected to uniform step loading σ_0 on crack faces is

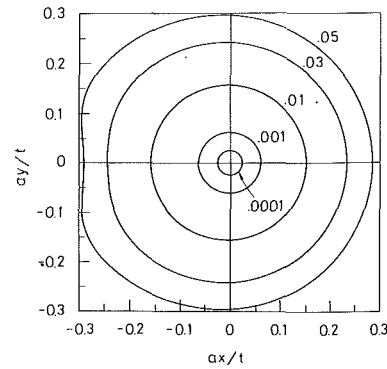


Fig. 1 Theoretical prediction of the initial curves from the dynamic transient stress field

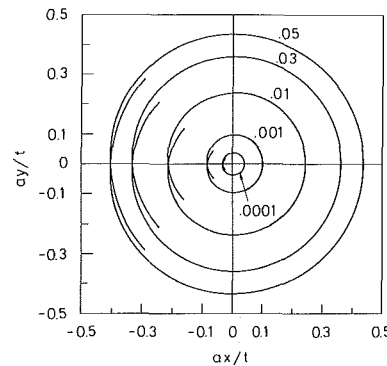


Fig. 2 Caustic curves from reflected light rays of the respective initial curves in Fig. 1

$$K(t) = 2 \sqrt{\frac{2}{\pi}} \sigma_0 \omega_0 t^{1/2}, \quad (2)$$

and

$$\omega_0 = \frac{\sqrt{a}}{cS_+(0)} = \frac{\sqrt{2a(b^2 - a^2)}}{b^2},$$

$$S_+(0) = \exp\left(-\frac{1}{\pi} \int_a^b \tan^{-1} \left[\frac{4y^2(y^2 - a^2)^{1/2}(b^2 - y^2)^{1/2}}{(b^2 - 2y^2)^2} \right] \frac{dy}{y}\right),$$

$$a = \sqrt{\frac{\rho}{\gamma + 2\mu}} = \frac{1}{v_l}, \quad b = \sqrt{\frac{\rho}{\mu}} = \frac{1}{v_s},$$

where μ and ρ are the shear modulus and the mass density of the material, γ is the Lamé elastic constant, a and b are the slowness of longitudinal and shear waves, respectively, and $c = 1/v_R$ is the slowness of Rayleigh wave.

The validity of the caustic scheme which can be used with acceptable accuracy is discussed by using the exact transient field of uniform impulse leading σ_0 in crack faces. The shapes of the initial curves and caustic curves in the transient field are determined numerically and are shown in Figs. 1 and 2. The values of parameter $\alpha (= \sigma_0 d \nu \omega_0 z_0 t^{1/2} / E)$ equal to 0.0001, 0.001, 0.01, 0.03, and 0.05 were chosen for the numerical calculation. For small values of α , the initial curve is close to the crack-tip region so that the deformation can be described by the singular field. The initial curves derived from the singular field should be circles with radii $r_i = [3\sigma_0 \omega_0 z_0 d \nu t^{1/2} / \pi E]^{2/5}$. As α becomes larger, the initial curve is distorted and is no longer circular. It is shown that, if the radius of the initial curve is about 0.1 ($\alpha \approx 0.01$) of the longitudinal wavefront ($ar/t = 1$), the initial curves are nearly circular.

The analysis of caustics is based on the assumption that the

⁹Professor, Department of Mechanical Engineering, National Taiwan University, Taipei 10764, Taiwan.

Manuscript received by the ASME Applied Mechanics Division, Oct. 4, 1988; final revision, Apr. 3, 1990.

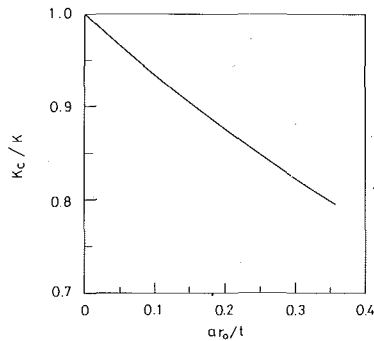


Fig. 3 Error in evaluation of the stress intensity factor by the method of caustics

stress singular field dominates in the region near the crack tip. Thus, it is important to estimate the resulting errors in evaluating the stress intensity factor by the caustic method under this assumption. A numerical simulation of the experimental observation is made by using the exact transient field for caustic mapping. By measuring the maximum transverse diameter of the caustic curve, the stress intensity factor K_c that would be calculated in an experiment on the basis of the observed caustic curve was evaluated through equation (1).

The theoretical value of the stress intensity factor K due to the uniform loading is given in (2). The ratio of the stress intensity factor K_c calculated from the caustic and K from the theoretical value is plotted as a function of the dimensionless parameter ar_0/t in Fig. 3. The initial curve radius r_0 is defined as the distance from the crack tip to the point of initial curve in x -axis. The deviation of K_c/K from unity indicates the error from using the singular field instead of the transient field to evaluate the stress intensity factors. Figure 3 shows that this error will be less than seven percent if the initial curve is within ten percent of the longitudinal wavefront.

3 Comparison With Experimental Results

In the work reported by Ravi-Chandar and Knauss (1984), a long edge crack was cut into a large rectangular sheet of Homalite-100 along a symmetrical line. The dimensions of the specimen were such that the waves generated by the loading device would not be reflected back onto the crack tip for about 150 μ sec after application of the pressure. Therefore, for all practical purposes, the situation is that of semi-infinite crack in an unbounded body subjected to spatially uniform pressure over the crack faces during the early part of the experiment. For the material of Homalite-100 as reported by Ravi-Chandar and Knauss (1984), only one caustic is observed in experiment, and thus it can be considered as a non-birefringent material. In this case, the formula for the reflected and transmission caustics are similar and are different only by a constant.

The theoretical analysis by Ma and Freund (1986) of the exact stress intensity factor for the experiment from the measured fracture time t_f , pressure magnitude σ_0 , crack propagation speed v and preload, was compared to the results reported by Ravi-Chandar and Knauss (1984). In all cases, the agreement between the theoretical and experimental results was found to be quite good for $t < t_f$ (the time for crack growth), with the general feature that the experimental data always fell below the theoretical prediction before the crack growth. With the available results discussed in the previous section, we are able to analyze in more detail for the time before crack propagation.

Up to this point in the theoretical analysis, it has been assumed that the time dependence of the loading pressure is a simple step in time. All of the results, however, can be generalized to the case of arbitrary stress profiles $g(t)$. Suppose that at time $t=0$, the crack pressure is applied, and that the

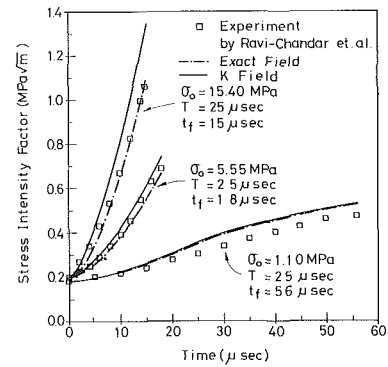


Fig. 4 The stress intensity factor history (solid lines) of the stationary crack from the loading observed in the experiments by Ravi-Chandar and Knauss (1984). Also shown is the stress intensity factor history inferred from the experimental results (data points) and the theoretical predictions (dash-dot lines) by means of the method of caustics.

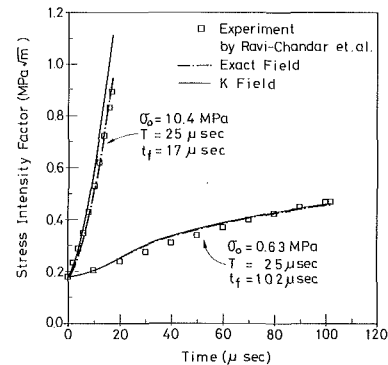


Fig. 5 Same as Fig. 4, but for data shown

magnitude of the pressure increases linearly. After some finite rise time T , the magnitude of the applied pressure reaches its maximum value σ_0 so that $g(T) = \sigma_0$. The magnitude of the pressure is held constant for $t > T$. The dynamic stress intensity factor of the stationary crack for $T < t_f$ is given by

$$K(t) = \frac{4\sqrt{2}\sigma_0\omega_0}{3\sqrt{\pi}T} [t^{3/2} - (t-T)^{3/2}H(t-T)], \quad 0 < t < t_f \quad (3)$$

When $t_f < T$, we have

$$K(t) = \frac{4\sqrt{2}\sigma_0\omega_0}{3\sqrt{\pi}T} t^{3/2}, \quad 0 < t < t_f \quad (4)$$

The size of the initial curve depends on the reference distance z_0 and also on the stress intensity factor. If the stress intensity factor were constant, the initial curve could be adjusted by changing the distance z_0 . However, if the stress intensity factor varies as in a dynamic experiment, one does not have close control over the radius of the initial curve, aside from limiting its variation through a judicious choice of the screen distance z_0 . One of the screen distances z_0 used by Ravi-Chandar and Knauss (1984), 168 cm, is adopted for numerical simulation.

We have compared experimental measurements obtained by using shadow spots with analytical results in Figs. 4 and 5. The analytically predicted variation of the stress intensity factor is presented by the solid and dash-dot lines. The solid lines are the theoretical prediction for the stress intensity factor history as presented in equations (3) and (4). The dash-dot lines were calculated by numerical simulation for the experimental observation of the caustic method by using the exact transient solutions. The transmission caustic formula is used for the numerical simulation in order to be consistent with the experimental measurement. Within the error of experimental measurement, the agreement between the theoretical prediction by using the transient solutions (dash-dot line) and the exper-

imental determination of the stress intensity factor is seen to be good. The dash-dot lines are always below the solid lines and more close to the experimental results. The results indicate that the method of caustic used in the experiment might underestimate the true stress intensity factor as the K -field is not developed at the measurement points. For the low magnitude of applied load, the dash-dot lines are very close to the solid line, which means that the initial curve for these cases are within the K -field and the difference from the theoretical value (solid-lines) is very small. For the high magnitude of loading, the situation is quite different, the initial curve is relatively large, the material points of initial curve are far away from the K -field, and hence the large difference from the theoretical prediction for the stress intensity factor is expected.

Another factor that might influence the accuracy of the method of caustic is that the theoretical results are within the framework of linear elastodynamics, while there must always be a zone of nonlinear and inelastic material response near the crack tip. One is not able to make meaningful measurements at very small distances from the crack tip where the stress field is significantly altered by the process zone for the determination of the dynamic stress intensity factor. Hence, the stress singular field possibly exists near the crack tip as an annular zone. The size of the process zone increases with increasing loading, resulting in a decrease of the annular region of the singular field. For higher load levels, this process zone may extend outward from the crack tip for a greater distance on the order of the initial curve size, in which case the assumption of linear elasticity would no longer be valid.

Acknowledgment

The research support of the National Science Council, Republic of China through Grant NSC78-0401-E002-28 at National Taiwan University is gratefully acknowledged.

References

- Ma, C.-C., and Freund, L. B., 1986, "The Extent of the Stress Intensity Factor Field During Crack Growth under Dynamic Loading Conditions," *ASME JOURNAL OF APPLIED MECHANICS*, Vol. 53, pp. 303-310.
- Ravi-Chandar, K., and Knauss, W. G., 1984, "An Experimental Investigation into the Mechanics of Dynamic Fracture: I. Crack Initiation and Arrest," *International Journal of Fracture*, Vol. 25, pp. 247-262; "II. Microstructural Branching," Vol. 26, pp. 141-154; "IV. On the Interaction of Stress Waves with Propagating Cracks," Vol. 26, pp. 189-200.
- Rosakis, A. J., and Freund, L. B., 1981, "The Effect of Crack Tip Plasticity on the Determination of Dynamic Stress Intensity Factors by the Optical Method of Caustics," *ASME JOURNAL OF APPLIED MECHANICS*, Vol. 48, pp. 302-308.
- Rosakis, A. J., and Zehnder, A. T., 1985, "On the Method of Caustics: An Exact Analysis Based on Geometrical Optics," *Journal of Elasticity*, Vol. 15, pp. 347-367.
- Rosakis, A. J., and Ravi-Chandar, K., 1986, "On Crack-Tip Stress State: An Experimental Evaluation of Three-Dimensional Effects," *Int. J. Solids Structures*, Vol. 22, pp. 121-134.

An Alternative Approach to the Symmetrical Top and Slender Member Analysis¹⁰

Nels Madsen¹¹

This Note considers the problem of a symmetrical top under the action of gravity, or analogously the problem of a long,

¹⁰Work supported by SCI Systems, Inc., under SCI Contract No. 93155, dated Nov. 30, 1989.

¹¹Associate Professor, Mechanical Engineering Department, Auburn University, Auburn University, AL 36849-3501.

Manuscript received by the ASME Applied Mechanics Division, Dec. 8, 1988; final revision, May 1, 1990.

slender, initially straight linearly elastic, circular cross-section member loaded only at its ends. A nonbody fixed coordinate system is used. The standard results are obtained without any explicit reference to a space-fixed coordinate system.

Introduction

The conventional analysis of a symmetrical top under the action of gravity uses a coordinate system fixed in the top (Scarborough, 1958). The standard analysis of a long, slender, initially straight, linearly elastic, circular cross-section member loaded only at its ends also uses a body-fixed coordinate system and leads to the same equations (Love, 1944). The typical approach to the resulting equations involves the use of Euler angles to relate the body fixed coordinate system to a system fixed in space. These angles and their derivatives can be expressed in terms of elliptic functions. The objective of this note is to show that these elliptic expressions for the top angular velocity, or equivalently, the curvature of the slender member, can be developed without the introduction of Euler angles by using a nonbody fixed coordinate system. This coordinate system is commonly used in the description of space curves (Willmore, 1959), but is less familiar in the dynamics arena. The conventional approach to the problem of the symmetrical top uses a body-fixed axis system with one axis parallel to the body axis of symmetry. The analogous coordinate system for the slender member has one axis tangent to the member centerline and the other two axes fixed in the member cross-section. The approach discussed here will use what are known as path or natural coordinates. Relative to the slender member problem this system shares the tangent axis with the conventional approach but the cross-sectional axes are not body fixed. The cross-sectional axes are in the directions of the local normal and binormal associated with the member center line. The corresponding axes in the symmetrical top problem are the top axis of symmetry, an axis perpendicular to both the axis of symmetry and the instantaneous angular velocity vector, and the third axis necessary to complete the right-handed orthogonal triad. Using this coordinate system the top angular velocity, or equivalently, the centerline curvature, can be derived directly from the kinetic equations without the introduction of supplementary geometrical information. In particular the results can be obtained working solely in the local coordinate system without any explicit reference to the space-fixed coordinate system. While this alternative derivation is primarily of academic interest, it is possible that the alternative coordinate systems used have utility in other dynamics and slender member problems. The remainder of the Note provides the development for the symmetrical top problem. An analogous development for the slender member problem is possible with appropriate reidentifications of the variables. These revised identifications are introduced during the development.

Equation Development

The objective of the analysis of the symmetrical top is the determination of the time variation of the top angular velocity. In this case that angular velocity vector will be expressed relative to a rotating coordinate system so one must also determine the angular velocity of this rotating reference system. The angular velocity vector of a symmetrical top can be broken into two components, one parallel to the top axis of symmetry, and the other perpendicular to that axis. Equation (1) expresses this relationship where \mathbf{k} represents the top axis of symmetry.

$$\boldsymbol{\omega} = \omega_r \mathbf{k} + \omega_p \mathbf{j} \quad (1)$$

In slender member theory, \mathbf{k} would represent the local tangent, \mathbf{j} the local binormal, ω_p the centerline curvature, and ω_r the member twist per unit length. The orthogonal triad defined by equation (1) is not body fixed; however, a body-fixed system